



**Self-Consistent Computation of Transport Barrier Formation by  
Fluid Drift Turbulence in Tokamak Geometry**

B. Scott, F. Jenko, A. G. Peeters, A. C-Y. Teo  
Max Planck Institut für Plasmaphysik  
Euratom Association  
D-85748 Garching bei München, Germany

## Abstract

### SELF-CONSISTENT COMPUTATION OF TRANSPORT BARRIER FORMATION BY FLUID DRIFT TURBULENCE IN TOKAMAK GEOMETRY

(1) Computations of turbulence from the electromagnetic gyrofluid model are performed in a flux surface geometry representing the actual MHD equilibrium of the ASDEX Upgrade edge flux surfaces. The transition to ideal ballooning seen in simple geometries as the plasma beta rises is suppressed, leaving the transport at quantitatively realistic levels. Computations for core parameters at half-radius geometry show significant contribution due to the finite beta electron dynamics, possibly removing the standard ITG threshold. (2) Strong inward vorticity transport in edge turbulence, resulting from ion diamagnetic flows, may lead to a build up of mean  $\text{ExB}$  vorticity fast enough to cause an H-mode transition. (3) Friction of mean ion flows against neutrals involves both toroidal and poloidal flow components, leading to a finite radial current due to a given  $\text{ExB}$  profile even with zero poloidal rotation.

## 1. Electromagnetic Gyrofluid Model, Tokamak Geometry

We report on numerical studies of tokamak edge turbulence, transport, and bifurcation phenomena which form part of the development towards a comprehensive, self-consistent description of the transport barrier formation process from first principles.

A necessary ingredient of any such model is a model for low frequency magnetised plasma drift dynamics which is as complete as possible. The current state of the art is the gyrofluid model, which in principle can incorporate all three of the principal ingredients of drift turbulence: ion temperature gradient (ITG) dynamics [1,2], drift Alfvén (DALF) dynamics of the passing electrons [3], and trapped electrons [4]. No model as yet has all three; we report the first results from a gyrofluid model containing DALF dynamics, showing its importance not only in the plasma edge but also to predominantly ITG turbulence in the core.

The formulation of an electromagnetic gyrofluid model is a straightforward extension of the standard one, dropping the requirement that the electrons behave adiabatically and allowing the parallel electric field to have an inductive part [5]. This adds kinetic Alfvén effects to the parallel dynamics of the electrons, following their evolution self consistently. The underlying dynamics is the same as in the fluid model [3,6], with the additions that dissipation is more properly handled and that finite Larmor radius effects (notably, polarisation) are treated to arbitrary order.

Flux surface geometry may be accurately treated with a flux tube model in an axisymmetric system provided separatrices are avoided [7]; here we add global consistency with the procedure and definitions in [8]. An equilibrium is computed using the HELENA code [9], the desired radius is picked out, the local metric is computed; and then the metric, curvature operator, magnetic field strength, and unit vector divergence are stored as functions of the parallel coordinate for use by the turbulence code. The ASDEX Upgrade model and parameter regime are shown in Fig. 1.

The results of using an accurate geometry can be striking. The more traditional ballooning coordinate model [7], basically a sheared slab model with curvature terms added, yields the ideal ballooning instability at values of the plasma beta below the experimentally observed L-to-H transition. One proposal to remedy this is to invoke diamagnetic stabilisation, but in the absence of a pedestal in the pre-transition L-mode this is not available. We find that the use of the ASDEX Upgrade equilibrium leads to a partial suppression of ideal ballooning, due to the increased shear but also to the shaping effects, a strong function of ellipticity. The transport is at realistic levels – total power through the  $s_{95}$  surface slightly above 3 MW for a typical pre-transition L-Mode situation. Finally, the dependence on collisionality is weak at ASDEX Upgrade parameters, with the local  $\nu_*$  at the boundary below which Braginskii thermal conduction breaks down and Landau damping takes over the dissipation. These results are summarised in Fig. 2. The parameter  $\hat{\beta} = (c_s q R / 2 v_A L_p)^2$  reflects the strength of drift wave dynamics relative to Alfvén transients (it is important to note that these couple to the electron pressure [3]), where  $L_p$  is the pressure scale length. In these terms the MHD parameter  $\alpha_M = -q^2 R \nabla \beta$  is 1 at  $\hat{\beta} \approx 8$  and the experimental transition is at  $\hat{\beta} \approx 20$ . The sharp transition at  $\hat{\beta} \approx 5$  is identified as the onset of ideal ballooning by means of mode structure diagnostics, especially the probability distribution of phase shifts of the component waves [5]. This is shown in Fig. 3.

Core parameters differ from the edge situation principally through the much smaller value of the scale ratio  $qR/L_p$ . Due to the higher beta, we still have  $\hat{\beta} \sim 1$  although the electron thermal speed is much faster than the drift wave phase velocities. This makes  $\nabla n$  rather than  $\nabla p_e$  important to the electron dynamics. We find that the combination of finite  $\eta_i^{-1} = d \log n / d \log T_i$  and finite  $\hat{\beta} \sim 1$  brings very strong Alfvén dynamics into the ITG mode system, due to the ability of the inductive electric field to oppose the static force imbalance given by the parallel gradients of the electron density and electrostatic potential. The passing electrons are therefore nonadiabatic, possibly able to completely remove the ITG threshold. Exploratory computations are shown in Fig. 4. This situation is almost completely collisionless. Interpretations concerning the transition from edge to core turbulence [10] will be strongly affected.

## 2. Vorticity Transport and Rotation Damping

As Fig 1 shows, we do not find a parameter transition one could apply to the L-to-H transition observed in tokamak edges, in contrast to other work [11]. The reasons for the discrepancy are yet unknown, but many possible causes (periodic boundary conditions, Braginskii thermal conduction, flux tube domain aspect ratio, and global consistency) have been ruled out. The present results have been obtained with several different numerical treatments of the Alfvén dynamics (upwinding, a predictor/corrector scheme), and with both the fluid [6] and gyrofluid [5] models. The likelihood that they are accurate is large.

We turn therefore to profile effects, particularly the self consistent interaction between turbulence, ExB rotation, and the density and temperature profiles. There is

much circumstantial evidence that the L-to-H transition involves all of these in concert [12]. One very promising result from the above computations is the existence of a significant inward transport of total ion vorticity. This has an obvious origin: gyroviscosity. The total vorticity is made up of ExB and diamagnetic components (in a gyrofluid model,  $n_e - n_i$ , where  $n_i$  is the gyrofluid ion density, not the total ion density which is equal to  $n_e$ ), but due to gyroviscosity it is advected by the ExB velocity alone. This breaks the symmetry which keeps the purely ExB Reynolds stress small on average at small scales. It is a necessary result that if  $\tilde{p}_i$  is isotropic at small scales, then the turbulent ExB transport of  $p_i$  radially outward implies the inward transport of  $\nabla_{\perp}^2 p_i$ . Then, since the profile of  $p_i$  responds according to its own equation, if these diamagnetic vorticity fluctuations build up a mean vorticity profile the latter will result in the form of an ExB rotation profile, which due to the accumulating mean vorticity will be sheared. This is basically a modification of the standard predator/prey scenario within the same paradigm [13]. Investigation of the self-consistent profile reaction to this vorticity transport by means of a nonlocal extension to the electromagnetic gyrofluid code is in progress.

Consideration of the ExB rotation profile will have to include the presence of neutral friction. Since this acts on both the toroidal and poloidal rotation components, one cannot consider solely poloidal rotation (the only component damped by neoclassical viscosity). We have attempted a detailed calculation of these effects in ASDEX Upgrade, taking the sheared rotation profile as given and applying Monte Carlo techniques to compute the net radial current induced by both neoclassical and neutral dissipation [14]. For solely poloidal flow the neutrals produce a small addition to the radial friction current [15]. With both toroidal and poloidal flow considered, the end state is zero poloidal flow and a balance between neutral friction and toroidal flow for the given ExB profile. However, the corresponding damping rate of the ExB vorticity is comparable to or smaller than the ion collision frequency, smaller than what one finds in the more collisional fluid regime in which one can use standard bulk viscosity [17]. It is therefore important to use expressions for damping that are well behaved in the weakly collisional regime [2], in which the edge as well as core regions of modern tokamaks find themselves.

### 3. Scrape Off Layer and Kinetic Effects

Earlier investigations of coupling between closed and open field line regions showed the transition between the two to be gradual, with a radial width of about 2 to 3 cm [18]. On open field lines in the scrape off layer (SOL) region, the turbulence character is much more interchange like due to the lack of field line connection – the driven range is at longer wavelength and the coupling between density and potential is much weaker due to the sheath conditions at the end of the field lines. This is not yet fully incorporated into the gyrofluid codes (but see [19], but our earlier experience with simplified models (zero fluctuations or zero parallel gradient at field line ends) shows much the same character as in [18]; without closed field line connection there is a  $\nabla_{\parallel} = 0$  component which behaves largely electrostatically.

A companion model to the fluid suite is our phase space drift kinetic electron code [20]. It has also been extended to include the kinetic Alfvén parallel dynamics that lie at the heart of the DALF system. Gyrokinetic ions for this code lie in the near future, but in the meantime several benchmarks with the Landau fluid DALF code have been carried out in the simple ballooning geometry. Transport at zero collisionality as a function of  $\beta$  agrees well with the fluid code, with the largest discrepancy at 0.4 versus 0.25 for the range  $1 < \beta < 10$ . The kinetic model also produces the ideal ballooning transition. The validity of the fluid models incorporating the simple Landau damping closures of [1,2] is helped by the fact that magnetic shear reduces the role played by wave/particle trapping of electrons moving along magnetic field lines [20]. Investigation of the validity of the ion Landau closure in the presence of the strong DALF dynamics at core parameters discussed above is urgently needed; this will be treated in the near future.

#### 4. Further Directions

Among the most critical things to do next is to build the gyrokinetic phase space code mentioned above. Techniques developed in gyrokinetic particle codes in current use will be applied to the gyrokinetic ion distribution function, which is tied to the electron function through the gyrokinetic polarisation equation [21]. Besides buttressing the gyrofluid model in the electromagnetic regime, this will provide a useful check on discreteness effects in the particle codes, especially in the representation of the higher-order moments appearing in the gyrofluid model. Electron trapping will be incorporated self consistently as well.

Another need is a nonlocal version of the gyrofluid model to treat self consistent pedestal physics, an electromagnetic gyrofluid version of [22]. Radial variations of the flux surface geometry in the edge are expected to have a significant effect on the spatial variation of the turbulence drive, transfer, and dissipation.

Interaction of the turbulent transport with the profiles and vice versa is another avenue gaining increasing attention. At the moment the DALF model results are being used as one of several components in a numerical function to give the transport in terms of background quantities, in the Multi Mode Model transport code [23]. It is also important to consider the self consistent dynamical evolution of the turbulence and transport, especially if the profiles change rapidly; it is also interesting to use coupled models to arrive at a global description, without paying penalties for machine size or the separation of time scales [24]. We plan to do this with the B2/EIRENE edge code [25] in the near term; self-consistent mean field treatment of the transport, as in [14] for the flow dynamics, will be necessary to include several anomalous thermal transfer effects as well as the basic transport of the profiles

#### References

- [1] DORLAND, W., HAMMETT, G.W., Phys. Fluids B **5** (1993) 812.
- [2] BEER, M.A., HAMMETT, G.W., Phys. Plasmas **3** (1996) 4046.

- [3] SCOTT, B., Plasma Phys. Control. Fusion **39** (1997) 1635.
- [4] BEER, M.A., HAMMETT, G.W., Phys. Plasmas **3** (1996) 4018.
- [5] SCOTT, B., "Electromagnetic Gyrofluid Turbulence in Tokamak Edge Geometries". Varenna Conference on Fusion Plasmas (1998).
- [6] SCOTT, B., Contrib. Plasma Phys. **38** (1998) 171.
- [7] BEER, M.A., COWLEY, S.C., HAMMETT, G.W., Phys. Plasmas **2** (1995) 2687.
- [8] SCOTT, B., Phys. Plasmas **5** (1998) 2334.
- [9] HUIJSMANS, G., "External resistive modes in tokamaks". Ph.D. thesis, Vrije Universiteit Amsterdam (1991)
- [10] ZEILER, A., HALLATSCHEK, K., *et al.* these Proceedings, paper IAEA-F1-CN-69 THP 2/02.
- [11] ROGERS, B., DRAKE, J.F., DORLAND, W., ZEILER, A., these Proceedings, paper IAEA-F1-CN-69 THP 2/01.
- [12] Plasma Phys. Control. Fusion **40** Special Issue: Papers from the 6th IAEA Technical Committee Meeting on H-mode Physics, no 5, pp 531-861.
- [13] DIAMOND, P.H., LIANG, Y.-M., CARRERAS, B.A., TERRY, P.W., Phys. Rev. Lett. **72** (1994) 2565.
- [14] PEETERS, A.G., Phys. Plasmas **5** (1998) 763.
- [15] PEETERS, A.G., Plasma Phys. Control. Fusion **40** (1998) 703.
- [16] SHANG, K.C., YOKOHAMA, M., WAKATANI, M., HSU, C.T., Phys. Plasmas **3** (1996) 965.
- [17] MCCARTHY, D.R., DRAKE, J.F., GUZDAR, P.N., HASSAM, A.B., Phys. Fluids B **5** (1993) 1188.
- [18] SCOTT, B., "Three Dimensional Computation of Collisional Drift Wave Turbulence and Transport in Tokamak Geometry", Proceedings of the 23rd EPS Conference on Controlled Fusion and Plasma Physics" (EPS, Kiev, 1996), a005, p 54.
- [19] XU, X., COHEN, R., *et al.* these Proceedings, paper IAEA-F1-CN-69 THP 2/03.
- [20] JENKO, F., SCOTT, B., Phys. Rev. Lett. **80** (1998) 4883.
- [21] PARKER, S.E., Lee, W.W., Phys. Plasmas **5** (1993) 77.
- [22] SCOTT, B., Plasma Phys. Control. Fusion **39** (1997) 471.
- [23] BATEMAN, G., KRITZ, A., *et al.* these Proceedings, paper IAEA-F1-CN-69 THP 2/19.
- [24] LODESTRO, L.L., *et al.* these Proceedings, paper IAEA-F1-CN-69 THP 2/04.
- [25] SCHNEIDER, R., COSTER, D.P., *et al.* these Proceedings, paper IAEA-F1-CN-69 THP 2/05.

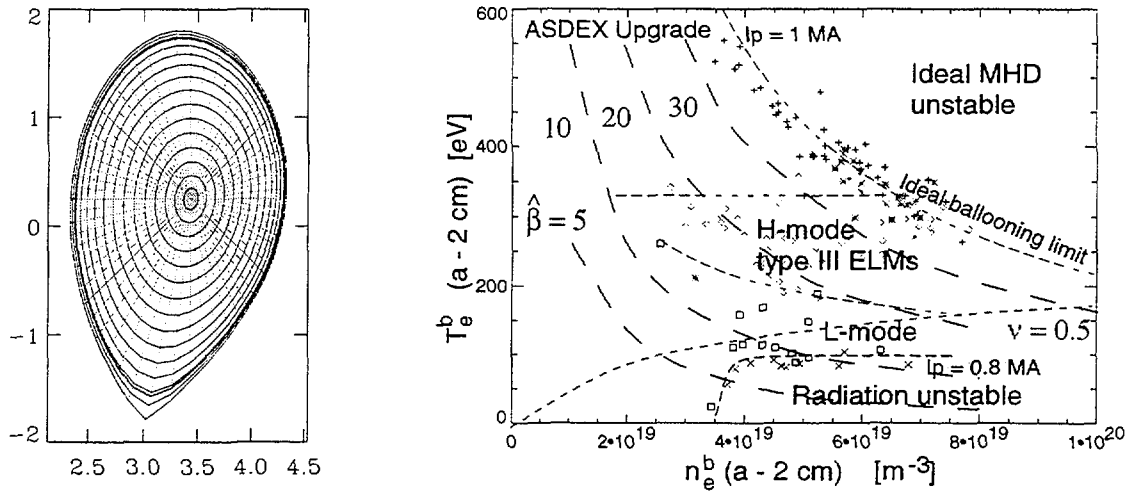


Fig. 1. (left) Flux surface geometry: the thick line denotes the  $s_{95}$  surface at which the edge fluxtube metric is calculated. The reference scale is 50 cm. (right) Edge parameter diagram, showing some of the  $\hat{\beta}$  values used, and the  $\nu = 0.5$  line.

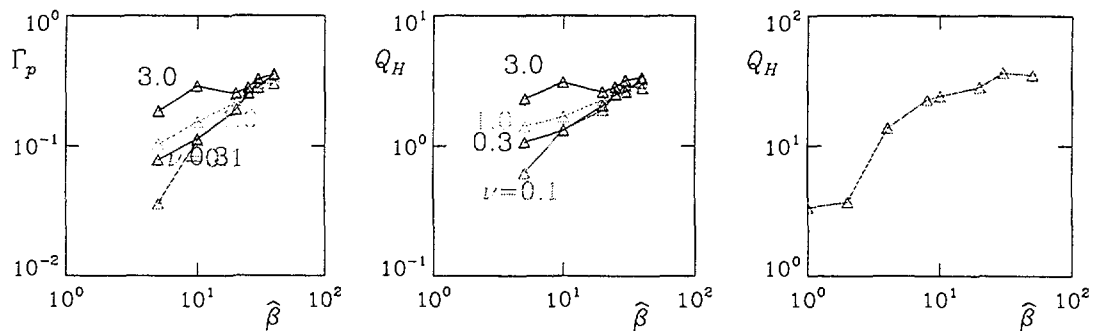


Fig. 2. Edge transport results. (left) particle and (center) total heat transport in the ASDEX Upgrade flux surface model, for several  $\hat{\beta}$  as a function of normalised collision frequency ( $\nu$  is about  $0.06 \times \nu_*$ ). Heat transport in the simple ballooning geometry (right) is strongly overestimated, especially by the appearance of ideal ballooning for  $\hat{\beta} > 5$ ; diagnosis is in the next figure.

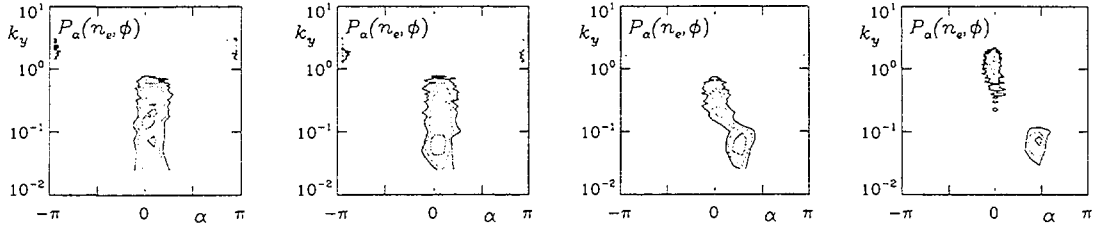


Fig. 3. Mode structure in the simple ballooning geometry, for (left to right)  $\hat{\beta} = 1.0, 2.0, 5.0,$  and  $10.0,$  respectively. Phase shifts ( $\alpha$ ) between the density and potential fluctuations for each component wave ( $k_y$ ), shown as probability distribution functions. Contours 0.3, 0.5, and 0.7 are shown. Drift wave mode structure (left) yields to ideal ballooning (drive at lowest  $k_y$ , followed by an inertial range) for  $\hat{\beta} > 5.0.$

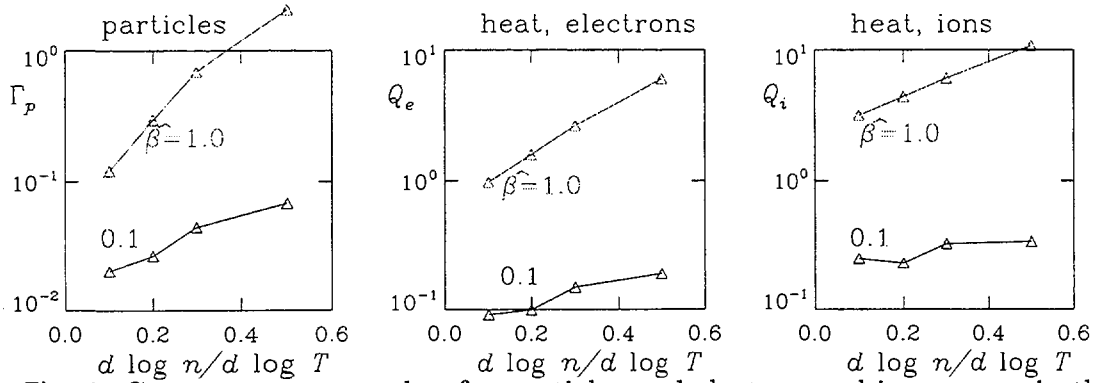


Fig. 4. Core transport results, for particles and electron and ion energy, in the ASDEX Upgrade flux surface model at the 0,6 normalised minor radius, for  $\hat{\beta} = 1.0$  (the actual value) and 0.1, showing the influence of  $\nabla n$  through the Alfvén dynamics. The value of  $\nu$  here is 0.01.

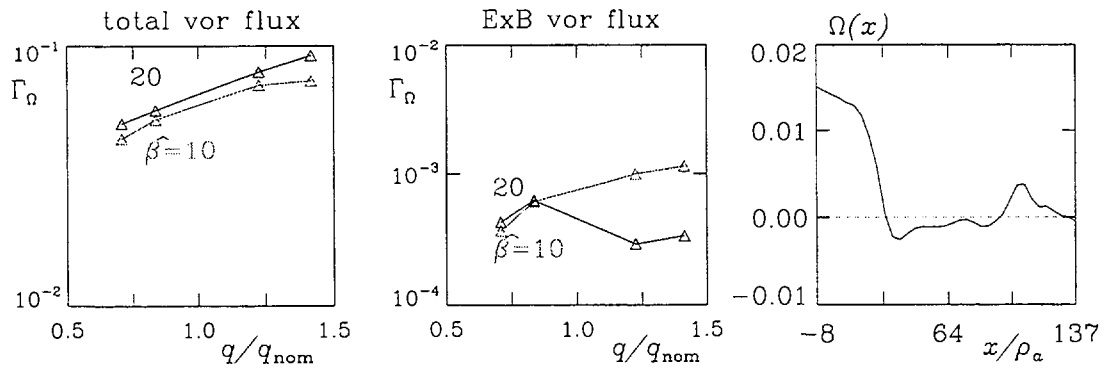


Fig. 5. Reynolds stress effects in the edge turbulence, preliminary result of the nonlocal model. (left) Inward diamagnetic vorticity transport, resulting from the outward ion heat transport. (center) The ExB Reynolds stress by itself is small. (right) Small scale diamagnetic vorticity builds up at the inside edge of a bounded domain, possibly leading to a strong ExB shear layer as at large scales the contribution of the diamagnetic to the total perpendicular flow is small.